The Journal of Chemical Physics

Ring-polymer, centroid, and mean-field approximations to multi-time Matsubara dynamics

Cite as: J. Chem. Phys. **153**, 124112 (2020); https://doi.org/10.1063/5.0021843
Submitted: 14 July 2020 . Accepted: 27 August 2020 . Published Online: 25 September 2020

Kenneth A. Jung, Pablo E. Videla, and Victor S. Batista

The Journal of Chemical Physics ARTICLE scitation.org/journal/jcp

Ring-polymer, centroid, and mean-field approximations to multi-time Matsubara dynamics

Cite as: J. Chem. Phys. 153, 124112 (2020); doi: 10.1063/5.0021843
Submitted: 14 July 2020 • Accepted: 27 August 2020 •
Published Online: 25 September 2020

Kenneth A. Jung,[a] Pablo E. Videla,[b] and Victor S. Batista

AFFILIATIONS

Department of Chemistry, Yale University, P.O. Box 208107, New Haven, Connecticut 06520-8107, USA

[a]**Current address:** Chemical Physics Theory Group, Department of Chemistry, and Center for Quantum Information and Quantum Control, University of Toronto, Toronto, Ontario M5S 3H6, Canada.
[b]**Author to whom correspondence should be addressed:** pablo.videla@yale.edu

ABSTRACT

Based on a recently developed generalization of Matsubara dynamics to the multi-time realm, we present a formal derivation of multi-time generalizations of ring-polymer molecular dynamics, thermostatted ring-polymer molecular dynamics (TRPMD), centroid molecular dynamics (CMD), and mean-field Matsubara dynamics. Additionally, we analyze the short-time accuracy of each methodology. We find that for multi-time correlation functions of linear operators, (T)RPMD is accurate up to order t^3, while CMD is only correct up to t, indicating a degradation in the accuracy of these methodologies with respect to the single-time counterparts. The present work provides a firm justification for the use of path-integral-based approximations for the calculation of multi-time correlation functions.

I. INTRODUCTION

Quantum thermal time correlation functions (TCFs) play a central role in the description of dynamical properties of chemical systems.[1–3] Despite recent advances in exact quantum solutions,[4–6] TCFs are still daunting to calculate exactly for condensed phase systems. In this regard, the development of semi-classical methodologies that include quantum statistical information yet employ classical dynamics show great promise. For single-time TCFs, which are relevant for understanding the linear response of systems,[7] Matsubara dynamics[8] has recently emerged as a leading theory that combines exact quantum-Boltzmann statistics with classical dynamics and satisfies detailed balance. Although not a practical theory due to the presence of a phase factor, Matsubara dynamics has provided a gateway to physical understanding[9,10] behind approximate path-integral-based methodologies such as (thermostatted) ring-polymer molecular dynamics[11–13] [(T)RPMD] and centroid molecular dynamics[14] (CMD). Moreover, Matsubara dynamics set the stage for the development of novel approximations.[15–17]

We recently developed an extension of Matsubara dynamics for the calculation of multi-time correlation functions,[18] which are implicated in the description of nonlinear spectroscopy[19,20] and nonlinear chemical kinetics.[21] As in the single-time case, the method involves a phase factor that makes it impractical, therefore, requiring further approximations for the computation of multi-TCFs in condensed phase systems. Based on the work done for the single-time case,[10,17,22,23] here we provide a formal derivation of different approximations to the multi-time Matsubara dynamics, including multi-time (T)RPMD, multi-time CMD, and multi-time mean-field (MF) Matsubara dynamics. This analysis gives a firm justification for the use of path-integral-based approximations for the calculation of multi-TCFs.[24,25] We also provide an analysis of the short-time error between the different multi-time approximations and Matsubara dynamics showing that the multi-time variants suffer a general loss in accuracy compared to the traditionally used single-time counterparts.

This article is organized as follows: the multi-time version of Matsubara dynamics is briefly described in Sec. II. Then, we introduce the derivation of RPMD, TRPMD, CMD, and a MF

approximation of Matsubara dynamics in Secs. III–VI, respectively. Numerical results showing the performance of each approximation for simple models are presented in Sec. VII. Final remarks are discussed in Sec. VIII.

II. MULTI-TIME MATSUBARA DYNAMICS

We consider a one-dimensional system of mass m with the Hamiltonian $\hat{H} = \frac{\hat{p}^2}{2m} + V(\hat{q})$ in which the observables $\hat{A}_i$ are assumed to be functions of position only. The generalization to multi-dimensional systems is straightforward.

We start by defining the fully symmetrized (imaginary-time ordered) nth order Kubo-transformed multi-time correlation function as[18,24]

$$K^{sym}(\boldsymbol{t}) \equiv \frac{1}{\beta^n}\int_0^\beta d\lambda_0 \int_0^\beta d\lambda_1 \cdots \int_0^\beta d\lambda_{n-1} \times \left\langle \hat{T}_\beta \hat{A}_0(-i\hbar\lambda_0)\hat{A}_1(-i\hbar\lambda_1 + t_1)\cdots \times \hat{A}_{n-1}(-i\hbar\lambda_{n-1} + t_{n-1})\hat{A}_n(t_n)\right\rangle, \tag{1}$$

where $\hat{O}(\tau) = e^{i\hat{H}\tau/\hbar}\hat{O}e^{-i\hat{H}\tau/\hbar}$, $\beta = 1/k_BT$ is the inverse temperature, $\hat{T}_\beta$ is an imaginary-time ordering operator that guarantees $\lambda_0 \geq \lambda_1 \geq \cdots \geq \lambda_{n-1}$ inside the integrals, and $\boldsymbol{t} = [t_1, t_2, \ldots, t_{n-1}, t_n]$ represents n independent time variables. The ensemble average in Eq. (1) is given by $\langle\cdot\rangle = Tr\left[\frac{e^{-\beta\hat{H}}}{Z}\cdot\right]$ with $Z = Tr\left[e^{-\beta\hat{H}}\right]$ being the partition function. The fully symmetrized Kubo transform is a real function of all time variables and shares many formal properties and symmetries with classical multi-TCFs.[18,25] When $n = 1$, Eq. (1) reduces to the single-time Kubo transform[7] that can be related through linear response theory to transport coefficients, reaction rates, and linear spectroscopy.[2,3,26–28] When $n = 2$, Eq. (1) gives the two-time symmetrized double Kubo transform[18,25] that has recently been related to second-order spectroscopy.[25]

The multi-time Matsubara approximation[8] to the fully symmetrized nth order Kubo transform TCF [Eq. (1)] is given by the $M \to \infty$ limit of[18]

$$K^{sym}_{Mats}(\boldsymbol{t}) = \frac{1}{(2\pi\hbar)^M Z_M}\int d\boldsymbol{Q}\int d\boldsymbol{P}\, e^{-\beta[H_M(\boldsymbol{Q},\boldsymbol{P}) - i\theta_M(\boldsymbol{Q},\boldsymbol{P})]} \times A_0(\boldsymbol{Q})\prod_{k=1}^{n} e^{\mathcal{L}_M(\boldsymbol{Q},\boldsymbol{P})t_k}A_k(\boldsymbol{Q}) \tag{2}$$

with the partition function

$$Z_M = \frac{1}{(2\pi\hbar)^M}\int d\boldsymbol{Q}\int d\boldsymbol{P}\, e^{-\beta[H_M(\boldsymbol{Q},\boldsymbol{P}) - i\theta_M(\boldsymbol{Q},\boldsymbol{P})]}, \tag{3}$$

the Matsubara Hamiltonian

$$H_M(\boldsymbol{Q},\boldsymbol{P}) = \frac{\boldsymbol{P}^2}{2m} + U_M(\boldsymbol{Q}), \tag{4}$$

the Matsubara phase

$$\theta_M(\boldsymbol{Q},\boldsymbol{P}) = \sum_{j=-\tilde{M}}^{\tilde{M}} P_j\omega_j Q_{-j}, \tag{5}$$

and the Matsubara Liouvillian given by

$$\mathcal{L}_M(\boldsymbol{Q},\boldsymbol{P}) = \sum_{j=-\tilde{M}}^{\tilde{M}} \frac{P_j}{m}\frac{\partial}{\partial Q_j} - \frac{\partial U_M(\boldsymbol{Q})}{\partial Q_j}\frac{\partial}{\partial P_j}. \tag{6}$$

In the previous equations, the coordinates $\boldsymbol{Q} = \{Q_j\}$, with $j = -\tilde{M}, \ldots, \tilde{M}$ and $\tilde{M} \equiv (M-1)/2$, are the positions of the M Matsubara modes[8] with frequency $\omega_j = 2\pi j/\beta\hbar$ (with similar definitions for momenta $\boldsymbol{P} = \{P_j\}$). Additionally, the smoothed Matsubara potential is given by

$$U_M(\boldsymbol{Q}) = \frac{1}{\beta\hbar}\int_0^{\beta\hbar} d\tau\, V(q(\tau)) \tag{7}$$

with the smoothed distribution of positions $q(\tau)$ constructed from the Matsubara modes as

$$q(\tau) = Q_0 + \sqrt{2}\sum_{j=1}^{\tilde{M}} \sin(\omega_j\tau)Q_j + \cos(\omega_j\tau)Q_{-j}. \tag{8}$$

Analogous definitions hold for the observables $A_k(\boldsymbol{Q})$.

The significance of Eq. (2) is that the dynamics generated by $\mathcal{L}_M$ is classical. Moreover, the Matsubara phase factor $e^{i\beta\theta_M}$ converts the classical Boltzmann distribution $e^{-\beta H_M}$ into the (exact) quantum Boltzmann distribution. Notice that since $\mathcal{L}_M H_M = \mathcal{L}_M\theta_M = 0$,[8] the quantum Boltzmann distribution is conserved during the classical evolution of the Matsubara modes and, therefore, the Matsubara multi-time correlation function obeys detailed balance.

Unfortunately, the presence of the phase factor in the Boltzmann distribution makes the convergence of the time correlation function very difficult, making Matsubara dynamics unpractical for simulations of large systems. For this reason, it is desirable to obtain practical approximations to Matsubara dynamics that allow for the inclusion of nuclear quantum effects in the simulation of condensed phase systems.

To avoid the difficulties associated with the complex Matsubara distribution, it is possible to perform the variable substitution[9,10,22,23]

$$P_j \to \tilde{P}_j + im\omega_j Q_{-j} \tag{9}$$

for each Matsubara mode to obtain

$$e^{-\beta[H_M(\boldsymbol{Q},\boldsymbol{P}) - i\theta_M(\boldsymbol{Q},\boldsymbol{P})]} \to e^{-\beta R_M(\boldsymbol{Q},\tilde{\boldsymbol{P}})} \tag{10}$$

where the ring-polymer Hamiltonian is given by

$$R_M(\boldsymbol{Q},\tilde{\boldsymbol{P}}) = \frac{\tilde{\boldsymbol{P}}^2}{2m} + S_M(\boldsymbol{Q}) + U_M(\boldsymbol{Q}) \tag{11}$$

with the polymer spring potential defined as

$$S_M(\boldsymbol{Q}) = \sum_{j=-\tilde{M}}^{\tilde{M}} \frac{1}{2}m\omega_j^2 Q_j^2. \tag{12}$$

Additionally, the change of variables allows one to rewrite the Liouvillian as $\mathcal{L}_M(\boldsymbol{Q},\boldsymbol{P}) \to \tilde{\mathcal{L}}_M(\boldsymbol{Q},\tilde{\boldsymbol{P}})$, where

$$\tilde{\mathcal{L}}_M(\boldsymbol{Q},\tilde{\boldsymbol{P}}) \equiv \mathcal{L}_{RP}(\boldsymbol{Q},\tilde{\boldsymbol{P}}) + i\mathcal{L}_I(\boldsymbol{Q},\tilde{\boldsymbol{P}}) \tag{13}$$

with

$$\mathcal{L}_{RP}(\boldsymbol{Q},\tilde{\boldsymbol{P}}) = \sum_{j=-\tilde{M}}^{\tilde{M}} \frac{\tilde{P}_j}{m}\frac{\partial}{\partial Q_j} - \left[\frac{\partial U_M(\boldsymbol{Q})}{\partial Q_j} + m\omega_j^2 Q_j\right]\frac{\partial}{\partial\tilde{P}_j} \tag{14}$$

and

$$\mathcal{L}_I(\mathbf{Q},\tilde{\mathbf{P}}) = \sum_{j=-\tilde{M}}^{\tilde{M}} \omega_j \left(\tilde{P}_j \frac{\partial}{\partial \tilde{P}_{-j}} - Q_j \frac{\partial}{\partial Q_{-j}} \right). \tag{15}$$

Note that with the change of variables [Eq. (9)], the integrals over momenta $\{\tilde{P}_j\}$ in Eq. (2) should be evaluated in the complex plane. However, provided the integrand remains analytic (i.e., free of singularities) in the complex plane,[9] one can perform a standard contour-integration using a rectangular contour extending from the real axis to lower half of the imaginary axis (see the supplementary material), giving[29]

$$K^{sym}_{Mats}(\boldsymbol{t}) = \frac{1}{(2\pi\hbar)^M Z_M} \int d\mathbf{Q} \int d\tilde{\mathbf{P}}\, e^{-\beta R_M(\mathbf{Q},\tilde{\mathbf{P}})} \times A_0(\mathbf{Q}) \prod_{k=1}^{n} e^{\tilde{\mathcal{L}}_M(\mathbf{Q},\tilde{\mathbf{P}})t_k} A_k(\mathbf{Q}). \tag{16}$$

Notice that the combined effect of the transformation [Eq. (9)] and analytic continuation is to effectively transfer a complex Matsubara distribution with real dynamics into a real ring-polymer distribution but with complex dynamics generated by $\mathcal{L}_{RP} + i\mathcal{L}_I$, resulting in a problem that is equally difficult to evaluate.[30,31] However, Eq. (16) has provided a starting point to introduce approximations to the dynamics for the single-time case[9,16,17] and will be generalized to the multi-time realm in what follows.

III. MULTI-TIME RPMD

The first approximation consists on discarding the imaginary part of the Liouvillian $\tilde{\mathcal{L}}_M(\mathbf{Q},\tilde{\mathbf{P}})$ in Eq. (16) to obtain a time correlation function with real distribution and real dynamics given by

$$K^{sym}_{RPMD}(\boldsymbol{t}) = \frac{1}{(2\pi\hbar)^M Z_M} \int d\mathbf{Q} \int d\tilde{\mathbf{P}}\, e^{-\beta R_M(\mathbf{Q},\tilde{\mathbf{P}})} \times A_0(\mathbf{Q}) \prod_{k=1}^{n} e^{\mathcal{L}_{RP}(\mathbf{Q},\tilde{\mathbf{P}})t_k} A_k(\mathbf{Q}), \tag{17}$$

which represents a multi-time extension of ring-polymer molecular dynamics with Matsubara frequencies.[25] Note that since $\mathcal{L}_{RP}R_M = 0$, the (classical) dynamics generated by $\mathcal{L}_{RP}$ conserves the ring-polymer Boltzmann distribution and, therefore, satisfies detailed balance. Moreover, at time $t = 0$, the RPMD function reduces to the exact result since in this limit approximations to the Liouvillian are irrelevant. Furthermore, since $\mathcal{L}_I$ does not affect the dynamics of the centroid (namely, $\mathcal{L}_I Q_0 = 0$), the RPMD approximation is also exact for operators that only depend on the centroid (i.e., linear operators) moving in a harmonic potential, where the dynamics of the Matsubara modes is fully decoupled from one another. Notice that the multi-time RPMD was first proposed based on heuristic arguments in Ref. 25 for the calculation of two-time symmetrized double Kubo-transformed correlation functions. The derivation presented in this paper provides a rigorous justification of the methodology and corroborates the results obtained in Ref. 25.

The similarity of Eqs. (16) and (17) allows for an analysis of the short-time error produced by neglecting the imaginary Liouvillian in the propagation. We emphasize that this analysis provides a formal short-time limit and is not necessarily indicative of the long-time accuracy of the method.[34] To this end, we closely follow Ref. 32 and expand the time-evolution operators as

$$e^{\mathcal{L}t_k} A_k = \sum_{l=0}^{\infty} \frac{t_k^l}{l!} \mathcal{L}^l A_k. \tag{18}$$

Performing the exponential expansion in Eqs. (16) and (17) and noticing that the Boltzmann distributions are the same in both the equations, the TCF can be written as a sum of terms of the form

$$\left\langle A_0 \left(t_1^{l_1} \mathcal{L}^{l_1} A_1\right) \left(t_2^{l_2} \mathcal{L}^{l_2} A_2\right) \left(t_3^{l_3} \mathcal{L}^{l_3} A_3\right) \cdots \right\rangle_{RP}, \tag{19}$$

where $\langle \cdots \rangle_{RP}$ represents the thermal average with respect to the distribution generated by R_M (we have omitted constant factors $l!$ for simplicity). Armed with Eq. (19), the short-time error of RPMD can be determined by looking for the first term in which $\tilde{\mathcal{L}}_M^l A_k \neq \mathcal{L}_{RP}^l A_k$.

We start the analysis by focusing on linear operators for which $A_k = Q_0$. It is straightforward to show that $\tilde{\mathcal{L}}_M^l Q_0 = \mathcal{L}_{RP}^l Q_0$ for the case $l \leq 3$ and that $\tilde{\mathcal{L}}_M^4 Q_0 \neq \mathcal{L}_{RP}^4 Q_0$ (see the supplementary material).[32] Note that since the times t_k are independent, these results can immediately be applied to Eq. (19) indicating that multi-time RPMD agrees with multi-time Matsubara dynamics up to t^3 in all time variables $\boldsymbol{t}$, namely, $(t_1^3, t_2^3, t_3^3, \ldots)$. For the case of nonlinear operators, the disagreement between the RPMD and Matsubara Liouvillian occurs at $l = 2$ (see the supplementary material), revealing that the multi-time RPMD TCF agrees with multi-time Matsubara dynamics TCFs up to order t^1 in all time variables $(t_1^1, t_2^1, t_3^1, \ldots)$.

Quite remarkably, for the case of one-time correlation functions, i.e., correlations in which only one time (say t_1) is involved, one can perform an integration by parts in Eq. (19) (see the supplementary material) to show that RPMD actually agrees with Matsubara dynamics up to t^6 (t^2) for linear (nonlinear) operators, a well-known result.[32–34] The novel insight is that this agreement also holds for one-time *higher-order* Kubo-transformed correlation functions[24] that involve all observables A_k but only one time variable. Since the latter type of correlation functions are involved in, for example, the quadratic response theory of vibrational energy relaxation for single-mode excitations,[35] and given the success of RPMD for the simulation of a wide range of problems in condensed phase systems,[36] the results obtained in this work postulate RPMD as a promising methodology to approximate one-time higher-order Kubo-transformed correlation functions.

IV. MULTI-TIME THERMOSTATTED RPMD

One disadvantage of discarding $i\mathcal{L}_I(\mathbf{Q},\tilde{\mathbf{P}})$ in Eq. (16) is that the oscillation frequencies of the non-centroid normal modes are artificially increased,[9] an effect that gives rise to the well-known problem of "spurious resonance contamination" in RPMD.[12,13,37] Motivated by the fact that the addition of a friction term in the dynamics of a harmonic oscillator reduces the oscillation frequency,[2] instead of discarding $i\mathcal{L}_I(\mathbf{Q},\tilde{\mathbf{P}})$ in the dynamics one can replace it by the (adjoint) white-noise Fokker–Planck operator[38]

$$\mathcal{A}^{\dagger}_{wn}(\tilde{\mathbf{P}}) = -\tilde{\mathbf{P}} \cdot \boldsymbol{\Gamma} \cdot \nabla_{\tilde{\mathbf{P}}} + \frac{m}{\beta} \nabla_{\tilde{\mathbf{P}}} \cdot \boldsymbol{\Gamma} \cdot \nabla_{\tilde{\mathbf{P}}}, \tag{20}$$

where the first term represents the "drag" produced by the $M \times M$ positive semi-definite friction matrix $\boldsymbol{\Gamma}$ and the second term corresponds to the stochastic "kicks."

Inserting Eq. (20) into Eq. (16), one obtains the approximation

$$K^{sym}_{TRPMD}(t) = \frac{1}{(2\pi\hbar)^M Z_M}\int d\boldsymbol{Q}\int d\tilde{\boldsymbol{P}}\, e^{-\beta R_M(\boldsymbol{Q},\tilde{\boldsymbol{P}})} \times A_0(\boldsymbol{Q})\prod_{k=1}^{n} e^{\mathcal{A}^{\dagger}_{RP}(\boldsymbol{Q},\tilde{\boldsymbol{P}})t_k}A_k(\boldsymbol{Q}) \tag{21}$$

with $\mathcal{A}^{\dagger}_{RP} \equiv \mathcal{L}_{RP} + \mathcal{A}^{\dagger}_{wn}$, which represents a multi-time version of TRPMD[13] with the Matsubara frequencies. Note that since $\mathcal{A}_{wn}e^{-\beta R_M} = 0$ (see the supplementary material), the dynamics generated by $\mathcal{A}^{\dagger}_{RP}$ conserves the ring-polymer Boltzmann distribution.[13,22] Moreover, by defining the friction matrix as $\boldsymbol{\Gamma}_{ij} = 2|\omega_j|\delta_{ij}$, one recovers the correct oscillation frequency of the normal modes in a harmonic potential,[10,13,39] therefore, mitigating the "spurious contamination" and improving over RPMD. Note that since $\omega_0 = 0$, the friction has no effect on the dynamics of the centroid. For practical implementations in general anharmonic potentials, a friction matrix of the form $\boldsymbol{\Gamma}_{ij} = 2\gamma|\omega_j|\delta_{ij}$ with $0.5 \le \gamma \le 1$ has shown to provide reasonable results for single-time correlation functions[13,22] and multi-time correlation functions.[25]

An analysis of the short-time error produced by replacing the imaginary Liouvillian with the white-noise Fokker–Planck operator can also be performed. Noticing that $\mathcal{A}^{\dagger}_{wn}$ involves momentum derivatives only and does not affect the centroid, it is straightforward to show that $(\mathcal{A}^{\dagger}_{RP})^l Q_0 = \mathcal{L}^l_{RP}Q_0$ for $l = 1, 2, 3$. This implies [via Eq. (19)] that the error of multi-time TRPMD with respect to Matsubara dynamics is the same as RPMD, namely, in the case of general multi-TCFs up to order t^3 for linear operators and up to order t^1 for nonlinear operators for all times and in the case of one-time correlation functions up to t^6 (t^2) for linear (nonlinear) operators.

V. MULTI-TIME CMD

For correlation functions involving observables that only depend on the centroid, namely, $A_k(\boldsymbol{Q}) = A_k(Q_0)$, an alternative approximation to Matsubara dynamics can be performed if one replaces the Matsubara Liouvillian by a centroid mean-field average of the form

$$\mathcal{L}_C(Q_0,P_0) = \frac{1}{(2\pi\hbar)^{M-1}Z_0}\int d\boldsymbol{Q}'\int d\boldsymbol{P}' \times e^{-\beta[H_M(\boldsymbol{Q},\boldsymbol{P})-i\theta_M(\boldsymbol{Q},\boldsymbol{P})]}\mathcal{L}_M(\boldsymbol{Q},\boldsymbol{P}), \tag{22}$$

where the primes denote integration over all Matsubara modes except the centroid modes Q_0 and P_0. In the previous equation, $Z_0 \equiv Z_0(Q_0, P_0)$ is defined by

$$Z_0(Q_0,P_0) = \frac{1}{(2\pi\hbar)^{M-1}}\int d\boldsymbol{Q}'\int d\boldsymbol{P}' e^{-\beta[H_M(\boldsymbol{Q},\boldsymbol{P})-i\theta_M(\boldsymbol{Q},\boldsymbol{P})]} = e^{-\beta\frac{P_0^2}{2m}}e^{-\beta W_0(Q_0)}, \tag{23}$$

where in the last line we have introduced the centroid potential of mean force defined by

$$W_0(Q_0) = -\frac{1}{\beta}\ln\left[\left(\frac{m}{2\pi\beta\hbar^2}\right)^{\frac{(M-1)}{2}}\int d\boldsymbol{Q}'\, e^{-\beta[U_M(\boldsymbol{Q})+S_M(\boldsymbol{Q})]}\right]. \tag{24}$$

An explicit evaluation of the mean-field average in Eq. (22) gives (see the supplementary material)[9,17]

$$\mathcal{L}_C(Q_0,P_0) = \frac{P_0}{m}\frac{\partial}{\partial Q_0} - \frac{\partial W_0(Q_0)}{\partial Q_0}\frac{\partial}{\partial P_0}. \tag{25}$$

By replacing the Matsubara Liouvillian with the centroid Liouvillian in Eq. (2) [or Eq. (16)], a multi-time extension of centroid molecular dynamics with the Matsubara frequencies can be obtained (see the supplementary material),

$$K^{sym}_{CMD}(t) = \frac{1}{(2\pi\hbar)^M Z_M}\int d\boldsymbol{Q}\int d\tilde{\boldsymbol{P}}\, e^{-\beta R_M(\boldsymbol{Q},\tilde{\boldsymbol{P}})} \times A_0(Q_0)\prod_{k=1}^{n} e^{\mathcal{L}_c(Q_0,P_0)t_k}A_k(Q_0) \tag{26}$$

$$= \frac{1}{2\pi\hbar Z_M}\int dQ_0\int dP_0\, e^{-\beta\left[\frac{P_0^2}{2m}+W_0(Q_0)\right]} \times A_0(Q_0)\prod_{k=1}^{n} e^{\mathcal{L}_c(Q_0,P_0)t_k}A_k(Q_0). \tag{27}$$

CMD is exact in the $t = 0$ limit for linear operators, and the centroid Boltzmann distribution is preserved by the dynamics generated by $\mathcal{L}_C$. Notice that the multi-time CMD was first introduced in Ref. 24 as a way of computing one-time correlation functions of non-linear operators and has been related to a path-integral expression of the vibrational energy relaxation for single-mode excitations.[35]

Comparing Eq. (26) with Eq. (16), we perform an analysis of the short-time error introduced by replacing the Matsubara Liouvillian with the centroid Liouvillian. Following a similar procedure as in Secs. III–IV, we expand the time-evolution operators to express the centroid TCF as sums of terms of the form (19) and look for the first term for which $\mathcal{L}^l_C A_k \neq \tilde{\mathcal{L}}^l_M A_k$. A direct analysis shows that $\mathcal{L}_C Q_0 = \tilde{\mathcal{L}}_M Q_0$, but $\mathcal{L}^2_C Q_0 \neq \tilde{\mathcal{L}}^2_M Q_0$. For a general multi-time correlation function, this result indicates that multi-time CMD agrees with multi-time Matsubara dynamics in all time variables up to order t^1, namely, $(t^1_1, t^1_2, t^1_3, \ldots)$. However, for the case of one-time correlation functions, a deeper analysis reveals that since only one Matsubara Liouvillian is involved in Eq. (19), the integrals over the non-centroid modes can be integrated out (see the supplementary material) to show that CMD actually agrees to order t^3 with Matsubara dynamics, indicating an increase in accuracy for one-time single and higher-order Kubo-transformed correlation functions.

VI. MEAN-FIELD MATSUBARA

In Sec. V, we have shown that CMD is less accurate than RPMD regardless of the number of time variables. However, CMD has the advantage over RPMD that it can be systematically improved upon. There is no need to perform the mean-field average over all the non-centroid modes in Eq. (22). In particular, one can mean-field over

a subset of only the most highly oscillatory modes to define different mean-field approximations. To be more precise, let us denote by $\boldsymbol{Q}_N = \{Q_0, Q_{\pm1}, \ldots, Q_{\pm\bar{N}}\}$ the subsets of $N < +M$ Matsubara modes [with $\bar{N} = (N-1)/2$] that will be included in the dynamics. One can therefore define a mean-field (MF) Matsubara Liouvillian of the form

$$\mathcal{L}_{MF}(\boldsymbol{Q}_N, \boldsymbol{P}_N) = \frac{1}{(2\pi\hbar)^{M-N} Z_{MF}} \int d\boldsymbol{Q}' \int d\boldsymbol{P}' \times e^{-\beta[H_M(\boldsymbol{Q},\boldsymbol{P}) - i\theta_M(\boldsymbol{Q},\boldsymbol{P})]} \mathcal{L}_M(\boldsymbol{Q},\boldsymbol{P}), \tag{28}$$

where the primes now denote integration over the $M-N$ high frequency Matsubara modes. In the previous equation, Z_{MF} is defined by

$$Z_{MF}(\boldsymbol{Q}_N, \boldsymbol{P}_N) = \frac{1}{(2\pi\hbar)^{M-N}} \int d\boldsymbol{Q}' \int d\boldsymbol{P}' e^{-\beta[H_M(\boldsymbol{Q},\boldsymbol{P}) - i\theta_M(\boldsymbol{Q},\boldsymbol{P})]} = e^{-\beta\frac{\boldsymbol{P}_N^2}{2m}} e^{i\beta\theta_M(\boldsymbol{Q}_N,\boldsymbol{P}_N)} e^{-\beta W_{MF}(\boldsymbol{Q}_N)}, \tag{29}$$

where the potential of mean force is given by

$$W_{MF}(\boldsymbol{Q}_N) = -\frac{1}{\beta} \ln\left[\left(\frac{m}{2\pi\beta\hbar^2}\right)^{\frac{(M-N)}{2}} \int d\boldsymbol{Q}' \times e^{-\beta[U_M(\boldsymbol{Q}) + S_M(\boldsymbol{Q}) - S_M(\boldsymbol{Q}_N)]}\right]. \tag{30}$$

An explicit evaluation of the mean-field average in Eq. (28) gives (see the supplementary material)[9,17]

$$\mathcal{L}_{MF}(\boldsymbol{Q}_N, \boldsymbol{P}_N) = \sum_{j=-\bar{N}}^{\bar{N}} \frac{P_j}{m} \frac{\partial}{\partial Q_j} - \frac{\partial W_{MF}(\boldsymbol{Q}_N)}{\partial Q_j} \frac{\partial}{\partial P_j}. \tag{31}$$

By making the replacement of the Matsubara Liouvillian by the mean-field Liouvillian in Eq. (2), and assuming that the observables only depend on the $\boldsymbol{Q}_N$ modes, the multi-TCF can be approximated by (see the supplementary material)

$$K_{MF}^{sym}(\boldsymbol{t}) = \frac{1}{(2\pi\hbar)^N Z_M} \int d\boldsymbol{Q}_N \int d\boldsymbol{P}_N \times e^{-\beta\left[\frac{\boldsymbol{P}_N^2}{2m} + W_{MF}(\boldsymbol{Q}_N)\right]} e^{i\beta\theta_M(\boldsymbol{Q}_N,\boldsymbol{P}_N)} \times A_0(\boldsymbol{Q}_N) \prod_{k=1}^{n} e^{\mathcal{L}_{MF}(\boldsymbol{Q}_N,\boldsymbol{P}_N)t_k} A_k(\boldsymbol{Q}_N), \tag{32}$$

which represents a multi-time extension of mean-field Matsubara dynamics.[17] It is straightforward to show that the dynamics generated by $\mathcal{L}_{MF}$ conserves the Boltzmann distribution $e^{-\beta\left[\frac{\boldsymbol{P}_N^2}{2m} + W_{MF} - i\theta_M\right]}$ (see the supplementary material). Note that for $N = 1$, Eq. (32) is equivalent to CMD. However, for $N > 1$, $N-1$ non-centroid fluctuation modes are included in the dynamics, therefore, improving upon CMD.[17] In the limit $N = M$, Matsubara dynamics is recovered.

It is worth noticing that Eq. (32) contains a phase factor and, therefore, suffers from the same sign problem as Matsubara dynamics [Eq. (2)]. This fact raises the question of the utility of the mean-field TCF for practical applications. Note, however, that since Eq. (32) only involves the N Matsubara modes with the lowest frequency, the phase factor $\theta_M(\boldsymbol{Q}_N, \boldsymbol{P}_N)$ will be less oscillatory than the full Matsubara phase factor $\theta_M(\boldsymbol{Q}, \boldsymbol{P})$ in Eq. (2). Moreover, for practical applications, including only the first fluctuation modes $Q_{\pm1}$ has been shown to produce great improvements over CMD (*vide infra*),[17] demonstrating the utility of the mean-field approximation.

VII. NUMERICAL RESULTS

To illustrate the different methodologies introduced in Secs. II–VI, we present comparisons for the calculation of two-time correlation functions in simple one-dimensional model potentials. We consider a particle with mass $m = 1$ in a quartic potential $V(q) = \frac{1}{4}q^4$ and evaluate the symmetrized double Kubo-transformed correlation $\langle\hat{q}^2\hat{q}(t_1)\hat{q}(t_2)\rangle$ and $\langle\hat{q}^2\hat{q}^2(t_1)\hat{q}^2(t_2)\rangle$ for a temperature $\beta = 2$ (atomic units are used throughout). Additionally, we evaluate the correlation $\langle\hat{q}^2\hat{q}^2(t_1)\hat{q}^2(t_2)\rangle$ for a particle in a harmonic potential at a lower temperature of $\beta = 4$. All simulations were performed in the (Matsubara) normal mode representation using an analytical form for polynomial potentials, as described in the supplemental information of Ref. 8.

Matsubara dynamics was performed employing the velocity-Verlet algorithm with a time step of 0.1 a.u. Momenta were sampled from a classical Boltzmann distribution every 20 a.u. The integration over the Matsubara phase was done by evaluating the ratio

$$K_{Mats}^{sym}(t_1, t_2) = \frac{\langle e^{i\beta\theta_M(\boldsymbol{Q},\boldsymbol{P})} A_0(\boldsymbol{Q}) e^{\mathcal{L}_M t_1} A_1(\boldsymbol{Q}) e^{\mathcal{L}_M t_2} A_2(\boldsymbol{Q})\rangle_M}{\langle e^{i\beta\theta_M(\boldsymbol{Q},\boldsymbol{P})}\rangle_M}, \tag{33}$$

where $\langle\cdot\rangle_M$ denotes sampling from the distribution $e^{-\beta H_M(\boldsymbol{Q},\boldsymbol{P})}$. A total of *circa* 10^8 configurations were necessary to converge the results for $M = 5$. Including additional modes or performing the simulations at a lower temperature makes the computation extremely challenging, highlighting the impractically of Matsubara dynamics. We remark that since Matsubara dynamics is exact for a harmonic oscillator, simulations for this potential were not performed.

CMD and mean-field Matsubara dynamics were performed by computing the mean-field force on the fly employing an adaptation for M modes of the partially adiabatic framework introduced in Ref. 40. In brief, the dynamical masses of the $(N-M)$ highest modes are re-scaled as $m_n = m(\omega_n/\Gamma)^2$, ensuring an adiabatic decoupling with the lowest N modes. Additionally, a Langevin thermostat with the friction coefficient $\gamma = 2\Gamma$ is attached to the mean-fielded modes to ensure proper sampling. An adiabatic separation of $\Gamma = 32M/\beta$ and a time step of 0.001 a.u. were employed.[17] The phase was integrated as

$$K_{MF}^{sym}(t_1, t_2) = \frac{\langle e^{i\beta\theta_M(\boldsymbol{Q}_N,\boldsymbol{P}_N)} A_0(\boldsymbol{Q}_N) e^{\mathcal{L}_{MF} t_1} A_1(\boldsymbol{Q}_N) e^{\mathcal{L}_{MF} t_2} A_2(\boldsymbol{Q}_N)\rangle_{MF}}{\langle e^{i\beta\theta_M(\boldsymbol{Q}_N,\boldsymbol{P}_N)}\rangle_{MF}}, \tag{34}$$

where $\langle\cdot\rangle_{MF}$ denotes sampling from the distribution $e^{-\beta\left[\frac{\boldsymbol{P}_N^2}{2m} + W_{MF}(\boldsymbol{Q}_N)\right]}$. Simulations were performed with $M = 5$ and $N = 1$ or $N = 3$ for CMD and mean-field Matsubara dynamics, respectively, and a total of 10^5 trajectories were needed to converge the results.

TRPMD simulations were performed employing a time step of 0.1 a.u. and attaching a Langevin thermostat with the friction coefficient $\gamma = 2\omega_n$ to each of the normal modes. A total of $M = 5$ and $M = 15$ were employed for simulations at $\beta = 2$ and $\beta = 4$, respectively.

In Fig. 1, we present cuts along selected slices of the two-time correlation $\langle \hat{q}^2 \hat{q}(t_1) \hat{q}(t_2) \rangle$ for the quartic potential at $\beta = 2$ obtained with the different methodologies. We have also included the exact result for comparison. (See the supplementary material for contour plots of the full 2D TCF.) For this relatively high temperature, all methodologies are very accurate at short-times, although the accuracy decreases as either t_1 or t_2 increases, with CMD and TRPMD approximations worsening at earlier times than Matsubara dynamics. Note that at zero time ($t_1 = t_2 = 0$) both TRPMD and Matsubara dynamics are exact, whereas CMD (as expected for a nonlinear TCF) is slightly incorrect. However, by including the first non-centroid modes in the dynamics (mean-field results), the zero time limit of CMD can be corrected and even the longer time accuracy increases significantly (see, for example, the bottom panel of Fig. 1). The reason for this is twofold: (i) At time zero, the inclusion of non-centroid modes in the evaluation of the nonlinear operator makes the $t = 0$ value closer to the exact result; (ii) for $t > 0$, the inclusion of additional Matsubara modes makes the dynamics more accurate. These results demonstrate the efficiency and advantage of the mean-field approximation.[17]

A more severe test of the performance of the different methods is provided by the evaluation of the nonlinear correlation $\langle \hat{q}^2 \hat{q}^2(t_1) \hat{q}^2(t_2) \rangle$, as presented in Fig. 2. At time $t = 0$, CMD deviates significantly from the exact quantum result; including additional non-centroid modes appreciably improves the short-time limit, bringing the dynamics in close agreement with the Matsubara result. Note also that while TRPMD captures the zero-time limit correctly, it fails to reproduce the intensity of the first oscillation, likely due to the neglect of phase coherences.[11,25] In this regard, Matsubara dynamics correctly reproduces the short-time limit (first two oscillations) before decorrelating.

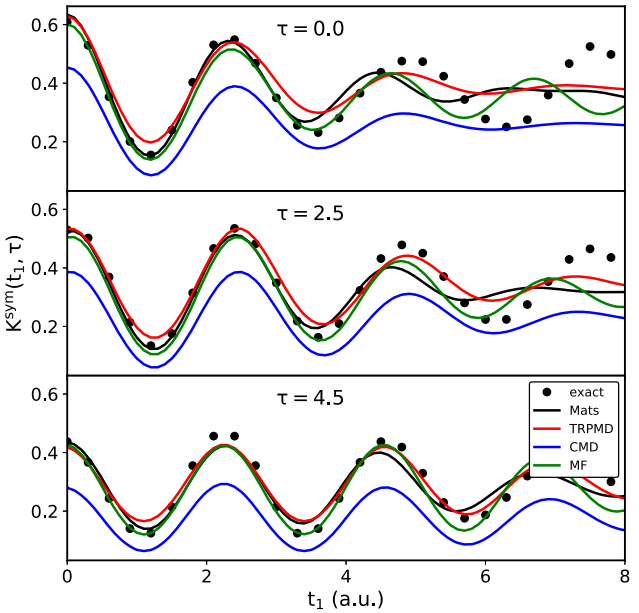

FIG. 2. Cuts along selected time slices for the symmetrized double Kubo-transformed $\langle \hat{q}^2 \hat{q}^2(t_1) \hat{q}^2(t_2) \rangle$ correlation function, for the quartic potential at $\beta = 2$, at different levels of theory.

Similar trends are observed at lower temperatures. In Fig. 3, we present results for the correlation $\langle \hat{q}^2 \hat{q}^2(t_1) \hat{q}^2(t_2) \rangle$ for a harmonic oscillator at $\beta = 4$. We remark that for the harmonic oscillator potential, Matsubara dynamics is exact for any

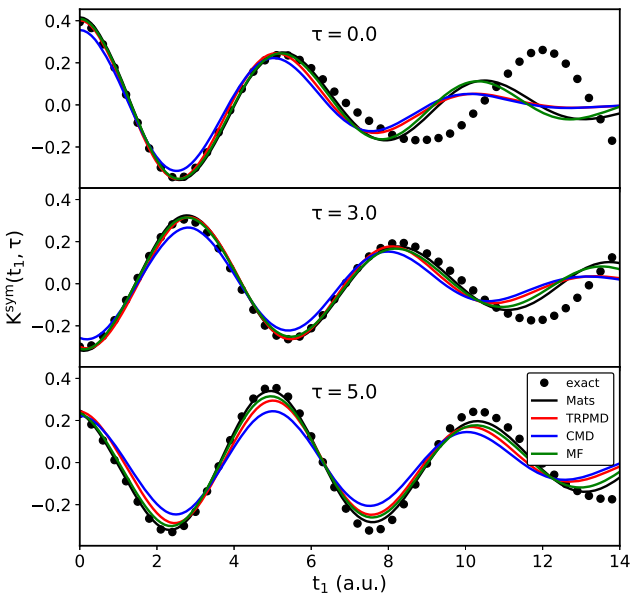

FIG. 1. Cuts along selected time slices for the symmetrized double Kubo-transformed $\langle \hat{q}^2 \hat{q}(t_1) \hat{q}(t_2) \rangle$ correlation function, for the quartic potential at $\beta = 2$, at different levels of theory.

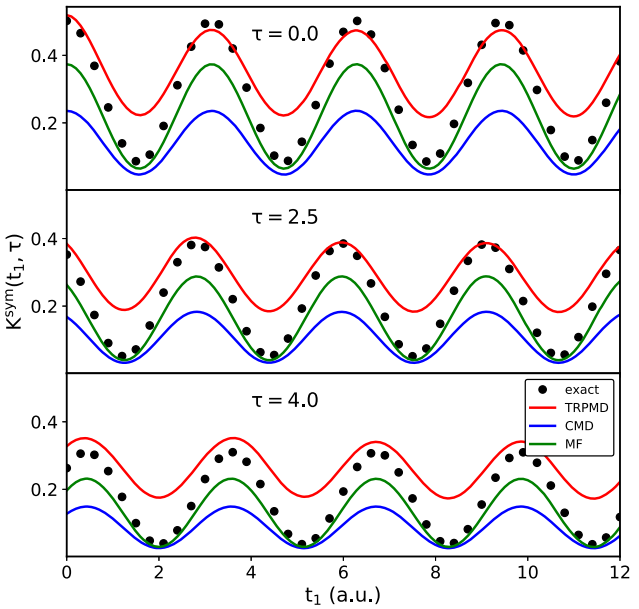

FIG. 3. Cuts along selected time slices for the symmetrized double Kubo-transformed $\langle \hat{q}^2 \hat{q}^2(t_1) \hat{q}^2(t_2) \rangle$ correlation function, for the harmonic potential at $\beta = 4$, at different levels of theory.

correlation function, whereas RPMD is exact for correlations with $\hat{A}_1 = \hat{A}_2 = \hat{q}$.[25] All methodologies correctly reproduce the oscillations but fail to reproduce the amplitude of the oscillations, though TRPMD starts at the correct value, whereas CMD is too low. Note that for this lower temperature, including the first non-centroid modes improves CMD, but additional modes are needed to converge the MF Matsubara dynamics even at time zero.

VIII. CONCLUSIONS

In the present work, we provided a formal justification for different path-integral-based semi-classical multi-time approximations, including (T)RPMD, CMD, and mean-field Matsubara dynamics, by relating these methods to multi-time Matsubara dynamics. Ring-polymer-based methods can be obtained by neglecting the imaginary part of the Matsubara Liouvillian (RPMD) or replacing it by white-noise stochastic dynamics (TRPMD). Mean-field methods (CMD and MF Matsubara) are obtained by averaging the Matsubara Liouvillian over a subset of non-centroid modes. All methodologies are exact at $t = 0$ (provided some approximations are fulfilled, i.e., linear operators for CMD) and generate approximate dynamics that conserve the quantum Boltzmann distribution.

Additionally, we have provided a short-time analysis of each method to check the agreement with Matsubara dynamics. We emphasize that this analysis provides a formal short-time limit and is not necessarily indicative of the long-time accuracy of the methods, which may depend on the underlying Hamiltonian, temperature, and type of correlation functions. For general multi-time correlation functions, we found that RPMD and TRPMD agree up to $O(t^3)$ in all times for linear operators and $O(t)$ for nonlinear operators. For one-time higher-order Kubo-transformed correlation functions, the agreement between (T)RPMD and Matsubara dynamics increases to $O(t^6)$ $[O(t^2)]$ for linear (non-linear) operators, such as in the one-time single Kubo-transformed TCF case. On the other hand, for linear operators, we found that CMD agrees with Matsubara dynamics up to $O(t)$ for multi-TCFs and up to $O(t^3)$ for single-TCFs. Numerical results demonstrate that by including additional modes in the mean-field dynamics a great improvement in the accuracy can be obtained. Given the connections of multi-time correlation functions and non-linear response functions,[19,25] the present work provides a firm justification for the use of path-integral-based approximations for the calculation of non-linear spectroscopy.[41]

SUPPLEMENTARY MATERIAL

The supplementary material contains detailed derivations of the main equations in the text and additional figures showing contour plots of the full 2D TCF.

ACKNOWLEDGMENTS

V.S.B. acknowledges support from NSF Grant No. CHE-1900160 and high-performance computing time from the Yale High Performance Computing Center.

DATA AVAILABILITY

The data that support the findings of this study are available within the article and its supplementary material.

REFERENCES

[1] D. Chandler, *Introduction to Modern Statistical Mechanics* (Oxford University Press, 1987).
[2] A. Nitzan, *Chemical Dynamics in Condensed Phases* (Oxford University Press, 2006).
[3] D. A. McQuarrie, *Statistical Mechanics* (University Science Books, 2000).
[4] H. Wang, J. Phys. Chem. A **119**, 7951 (2015).
[5] S. M. Greene and V. S. Batista, J. Chem. Theory Comput. **13**, 4034 (2017).
[6] G. W. Richings and S. Habershon, J. Chem. Phys. **148**, 134116 (2018).
[7] R. Kubo, J. Phys. Soc. Jpn. **12**, 570 (1957).
[8] T. J. H. Hele, M. J. Willatt, A. Muolo, and S. C. Althorpe, J. Chem. Phys. **142**, 134103 (2015).
[9] T. J. H. Hele, M. J. Willatt, A. Muolo, and S. C. Althorpe, J. Chem. Phys. **142**, 191101 (2015).
[10] T. J. H. Hele, Mol. Phys. **114**, 1461 (2016).
[11] I. R. Craig and D. E. Manolopoulos, J. Chem. Phys. **121**, 3368 (2004).
[12] S. Habershon, D. E. Manolopoulos, T. E. Markland, and T. F. Miller, Annu. Rev. Phys. Chem. **64**, 387 (2013).
[13] M. Rossi, M. Ceriotti, and D. E. Manolopoulos, J. Chem. Phys. **140**, 234116 (2014).
[14] J. Cao and G. A. Voth, J. Chem. Phys. **101**, 6168 (1994).
[15] K. K. G. Smith, J. A. Poulsen, G. Nyman, and P. J. Rossky, J. Chem. Phys. **142**, 244112 (2015).
[16] M. J. Willatt, M. Ceriotti, and S. C. Althorpe, J. Chem. Phys. **148**, 102336 (2018).
[17] G. Trenins and S. C. Althorpe, J. Chem. Phys. **149**, 014102 (2018).
[18] K. A. Jung, P. E. Videla, and V. S. Batista, J. Chem. Phys. **151**, 034108 (2019).
[19] S. Mukamel, *Principles of Nonlinear Optical Spectroscopy* (Oxford University Press, 1995).
[20] M. Cho, *Two-Dimensional Optical Spectroscopy* (CRC Press, 2009).
[21] M. Kryvohuz and S. Mukamel, J. Chem. Phys. **140**, 034111 (2014).
[22] T. J. H. Hele and Y. V. Suleimanov, J. Chem. Phys. **143**, 074107 (2015).
[23] T. J. H. Hele, Mol. Phys. **115**, 1435 (2017).
[24] D. R. Reichman, P.-N. Roy, S. Jang, and G. A. Voth, J. Chem. Phys. **113**, 919 (2000).
[25] K. A. Jung, P. E. Videla, and V. S. Batista, J. Chem. Phys. **148**, 244105 (2018).
[26] T. Yamamoto, J. Chem. Phys. **33**, 281 (1960).
[27] R. Zwanzig, Annu. Rev. Phys. Chem. **16**, 67 (1965).
[28] W. H. Miller, S. D. Schwartz, and J. W. Tromp, J. Chem. Phys. **79**, 4889 (1983).
[29] Strictly speaking, Eq. (16) should contain the edge terms of the contour integration. In what follows, we will assume that there are zero, which is the case for a variety of physical relevant Hamiltonians (see Ref. 10).
[30] C. M. Bender, D. C. Brody, and D. W. Hook, J. Phys. A: Math. Theor. **41**, 352003 (2008).
[31] G. Aarts, E. Seiler, and I.-O. Stamatescu, Phys. Rev. D **81**, 054508 (2010).
[32] R. Welsch, K. Song, Q. Shi, S. C. Althorpe, and T. F. Miller, J. Chem. Phys. **145**, 204118 (2016).
[33] B. J. Braams and D. E. Manolopoulos, J. Chem. Phys. **125**, 124105 (2006).
[34] S. Jang, A. V. Sinitskiy, and G. A. Voth, J. Chem. Phys. **140**, 154103 (2014).
[35] J. A. Poulsen, G. Nyman, and P. J. Rossky, J. Chem. Phys. **117**, 11277 (2002).
[36] S. Habershon, G. S. Fanourgakis, and D. E. Manolopoulos, J. Chem. Phys. **129**, 074501 (2008).
[37] A. Witt, S. D. Ivanov, M. Shiga, H. Forbert, and D. Marx, J. Chem. Phys. **130**, 194510 (2009).
[38] R. Zwanzig, *Nonequilibrium Statistical Mechanics* (Oxford University Press, 2001).
[39] M. Ceriotti, M. Parrinello, T. E. Markland, and D. E. Manolopoulos, J. Chem. Phys. **133**, 124104 (2010).
[40] T. D. Hone, P. J. Rossky, and G. A. Voth, J. Chem. Phys. **124**, 154103 (2006).
[41] Z. Tong, P. E. Videla, K. A. Jung, V. S. Batista, and X. Sun, J. Chem. Phys. **153**, 034117 (2020).